



## Prediction of Local Seismic Damage in Jacket-type Offshore Platforms

M. Aghajani Delavar, K. Bargi\*

School of Civil Engineering, College of Engineering, University of Tehran, Tehran, Iran

**ABSTRACT:** Due to the severe environmental condition, steel jacket type offshore platforms are highly vulnerable to damage; so, ensuring its proper performance and detection of probable damage is very important and undeniable. The assessment of existing offshore platforms is relatively a new process and has not yet been standardized as the design has. To do so, seismic assessment of the existing 4-legged steel jacket type offshore platform placed in the Persian Gulf (SPD12) is presented in this paper. Based on an actual platform structure and its mechanical model, the parameters which may affect the rate of shock absorption are analyzed, such as the condition of the site where the platform is located. Assessment is done by finding the seismic damage spread in the structure. Therefore, by using some documents such as FEMA-356 and ATC-40 developed for seismic assessment of buildings, seismic damage of the jacket-type platform is predicted with pushover analysis, and damage spread in this structure is predicted. This method could be very simple and detect damage spread precisely. As a result, knowing the weaker points of the structure which will be the first and third levels of the platforms similar to SPD12 in structural system can help to detect the damaged places, and by improving the capacity of the structure locally, the structural damage spread will be delayed.

### Review History:

Received: 22 July 2018

Revised: 9 September 2018

Accepted: 11 September 2018

Available Online: 24 September 2018

### Keywords:

Platform

Seismic Assessment

Offshore

Jacket

Damage Detection

### 1- Introduction

Structural steel is widely used in jacket-type offshore platforms. One of the most significant applications of offshore platforms is the oil/gas production from reservoirs below the sea bed. Fixed jacket-type platforms have usually been installed in shallower water about less than 100 m and are subjected to different environmental loads such as wind, current, wave, earthquake, snow, ice, and earth movement. Many offshore platforms have been installed in seismically active regions of the world's oceans. So, considering the effects of seismic loads on offshore platforms may improve the design procedure and make the structure more economic. Moreover, structural framing will be designed for ductile behavior and will avoid reduction of capacity resulting from damage, corrosion or fatigue.

Assessment of jacket platforms has seldom been studied, although the assessment process of building has been studied a lot. Malekpour et al. [1] discussed the advantages and disadvantages of codes by studying four 2-D steel moment resisting frame buildings with 3, 6, 9, and 12 stories with intermediate ductility levels designed using three different codes, then these structures are evaluated with FEMA-356 and ATC-40 provisions. Sultana and Youssef [2] proposed a simplified method to define the failure inter-story drift for each floor of a steel moment resisting frames (SMRFs), and this method is validated with the experimental and analytical studies by other researchers. At the end, the proposed method

identified the severely damaged floors of SMRFs precisely. McCrum and Staino [3] presented a new approach for global detection of seismic damage in a single-story steel concentrically braced frame (CBF) structure. Gholizadeh and Poorhoseini [4] utilized bat algorithm (BA) to implement performance-based optimum seismic design of steel dual braced frames for various performance levels. Moreover, there are some researches on assessing jacket platforms. Kringer et al. [5] illustrated the process of assessment of existing platforms. Golafshani et al. [6] suggested for the first time at 2006 that building documents can evaluate and improve the assessment of jacket platforms. Golafshani et al. [7] compared the comments of API with a detailed method of FEMA for seismic assessment of jacket platforms. Kim and Stubbs [8] described an algorithm to detect damage in jacket-type offshore structures. Yang et al. [9] presented a novel developed damage localization method. Shi et al. [10] proposed an algorithm based on partial measurement of vibration for offshore jacket platforms to detect damage. Elshafey et al. [11] detect damage in offshore jacket platforms subjected to random loads by combined method of random decrement signature and neural networks. Asgarian et al. [12] predicted damage location of jacket-type platforms by changing in modal strain energy ratio of elements. Asgarian et al. [13] proposed a method which can be used for prediction of damage in jacket-type platforms using wavelet packet transform. However, all of these researches are not simple and need much work to obtain the results. In this study, a new method for predicting damage location in jacket-type offshore platform is proposed to evaluate the structure efficiently.

Corresponding author, E-mail: kbargi@ut.ac.ir

This simple method can help to design this structure safer by detecting the initial damage under loads.

## 2- Case study

### 2- 1- Description of the jacket platform

In this research, a 3-D model of SPD12 jacket platform located in South Pars Gas Field of Persian Gulf region is employed as a case study. General configuration of SPD12 jacket platform is shown in Figure 1. It is located about 100 km offshore in the Persian Gulf [14]. Since the design of this platform is as same as other South Pars Gas Field platforms, the results of this study can be valid for other jacket structures with the same physical configuration in this area of Persian Gulf.

The well-head SPD12 platform consists of 4 main legs located in 71.4 m water depth. Jacket plan dimension is about 20.50 m × 24.25 m at deck level and 33.25 m × 38.50 m at mudline elevation. The jacket is fixed to the ground by 4 piles. The topside of the platform is made with two separate structures; main module and Free Water KO drum module (FWKO module). The main module consists of four decks, and the FWKO module consists of three decks.



Figure 1. Perspective plot of SPD12 jacket platform [14]

### 2- 2- Computer model

The dynamic model of fixed platforms should contain analytical parameters of mass, damping and stiffness. The 3-D model of SPD12 jacket-type platform is modeled in accordance with AS-BUILT drawings. The main elements of the structure are modeled to obtain the real stiffness, and the loads of other elements are assigned to the structure to have approximately the real mass. By these two parameters which play prominent roles in calculating the period of structure, the model of structure is verified by the real platform.

Analytical model is created using the SAP2000 software [15] which is more powerful in analyzing such a complex model than other software and useful for modeling of tubular members and assignments of nonlinear behavior of elements due to its user-friendly modeling. The dynamic model of fixed platforms should contain analytical parameters of mass, damping, and stiffness [16]. Due to the importance of loads in modeling of the structure, the equivalent existing loads such as weight of pile (above mudline), barge bumpers, boat landing, conductors, marine growth, added masses, live loads, and all of loads which exist on decks are assigned to the structure. The mass used in dynamic analysis should contain

the mass of the platform associated with gravity loading including the platform dead weight, actual live loads and 75% of the maximum supply and storage loads [16]. Moreover, additional moment due to P-Δ effects is considered for the weight of the deck.

Furthermore, for considering the soil-pile interaction, the equivalent length method is used to simplify the model of the structure. The suggested value for the equivalent length of the pile in loose clayey soils is 8D-12D, where D is the diameter of the pile [17]. In this research, a value of 12D, approximately equal to 18.3 m, is chosen as the equivalent length of the piles. For considering the water-structure interaction, the added mass is assigned to the elements with respect to the added mass coefficients. Added mass is the mass of water supposed in unison with the structural members as it deflects. For tubular members, a value of mass numerically equal to the mass of water displaced by the submerged member is used including marine growth where applicable. Figure 2 and Table 1 show the added mass coefficients as a function of submergence. The value for the vertical added mass coefficient is the same as that for the horizontal one when the tubular element is fully submerged, i.e. when  $d > D$  [18].

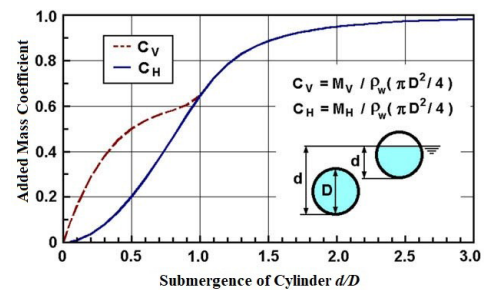


Figure 2. Vertical and horizontal added mass coefficients of cylinder as a function of submergence ratio  $d/D$  [18]

### 2- 3- Material properties

The properties of the steel used for modeling of the platform are presented in Table 2 and the differences due to the nominal thickness of the elements are presented in Table 3. In order to consider the material non-linearity, bilinear stress-strain curve with 3% of the elastic slope with maximum ductility of 14 is modeled for the member's behavior (Figure 3).

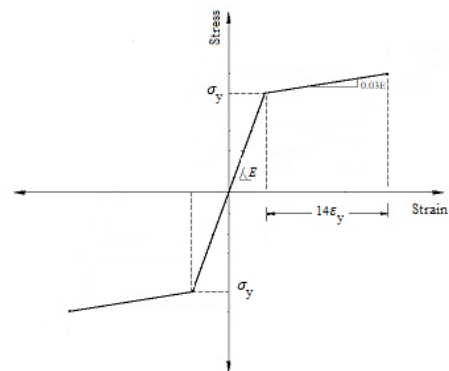


Figure 3. Steel material

**Table 1. Buoyancy and added mass coefficients of cylinder [18]**

| Submergence ratio<br>d/D | Buoyancy/ $\rho_w g A$<br>where $A = \pi D^2/4$ | Added mass coefficient                        |   |
|--------------------------|---|---|---|
|                          |   | Vertical<br>$C_V = M_V / \rho_w A \ddot{u}_z$ | Horizontal<br>$C_H = M_H / \rho_w A \ddot{u}_x$ |
| 0.1                      | 0.052   | 0.163   | 0.009   |
| 0.2                      | 0.142   | 0.286   | 0.036   |
| 0.5                      | 0.500   | 0.500   | 0.203   |
| 0.8                      | 0.858   | 0.581   | 0.461   |
| 1.0                      | 1.000   | 0.646   | 0.646   |
| 1.2                      | 1.000   | 0.783   | 0.783   |
| 1.5                      | 1.000   | 0.885   | 0.885   |
| 2.0                      | 1.000   | 0.948   | 0.948   |
| 3.0                      | 1.000   | 0.983   | 0.983   |

**Table 2. Steel properties**

|                 |                        |
|-----------------|------------------------|
| Grade           | S355                   |
| Density         | 7850 kg/m <sup>3</sup> |
| Young's Modulus | 200 GPa                |
| Poisson's Ratio | 0.3                    |

**Table 3. Yield stress of steel (N/mm<sup>2</sup>)**

| Nominal thickness in mm |     |     |     |      |      |
|-------------------------|-----|-----|-----|------|------|
| ≤16                     | >16 | >40 | >63 | >80  | >100 |
|                         | ≤40 | ≤63 | ≤80 | ≤100 | ≤150 |
| 350                     | 345 | 335 | 325 | 315  | 295  |

**2- 4- Modal analysis**

A modal analysis is performed on the platform using SAP2000 to extract the mode shapes of structural free vibration and the corresponding periods with considering P-Δ effect. The first three mode shapes are shown in Figure 4.

In order to verify the model, first 12 periods of the generated model are compared with the corresponding periods of SPD12 platform. Table 4 shows that the first two periods of the model are very close to the corresponding periods of the structure and other periods have a variation about 10% in average due to the simplification of the model.

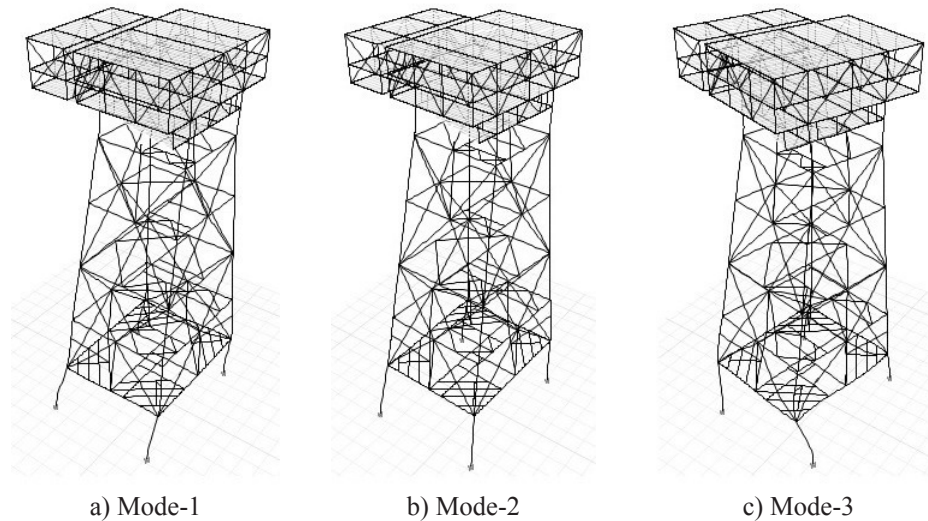


**Figure 4. First three mode Shapes of free vibration**

**Table 4. Comparison of periods**

| Mode | Modal Period | SPD12 Period | Error (%) |
|------|--------------|--------------|-----------|
| 1    | 2.957        | 3.004        | 1.5       |
| 2    | 2.506        | 2.565        | 2.3       |
| 3    | 2.081        | 1.638        | -27.0     |
| 4    | 1.179        | 0.974        | -21.0     |
| 5    | 1.145        | 0.945        | -21.0     |
| 6    | 0.738        | 0.739        | 0.1       |
| 7    | 0.455        | 0.533        | 14.6      |
| 8    | 0.415        | 0.531        | 21.8      |
| 9    | 0.403        | 0.500        | 19.4      |
| 10   | 0.341        | 0.341        | 0.0       |
| 11   | 0.292        | 0.308        | 5.2       |
| 12   | 0.279        | 0.286        | 2.4       |

**3- Numerical study**

Assessment of the structure and finding the location of damage is obtained with respect to FEMA recommendations. In this process, considering buoyancy force is essential to

obtain the correct response of the structure. This force is assigned to the elements under water and has the opposite direction in comparison with the gravitational loads. It can be calculated as shown in Equation 1.

$$F_B = \rho_f V_f g \tag{1}$$

Where  $F_B$  is buoyant force;  $\rho_f$  is density of the displaced water which is  $1025 \text{ kg/m}^3$ ; and  $V_f$  is volume of the displaced water, so it depends on the diameter of the section.

FEMA [19] and ATC [20] have fully described performance based design in their guidelines. There are four levels of building performance consisting of Operational (O), Immediate Occupancy (IO), Life Safety (LS), and Collapse Prevention (CP) [19]. The meaning of each level is fully illustrated in FEMA.

Due to the fully restrained moment frames and concentric braced frames of the platform, modeling parameters and numerical acceptance criteria for beams, columns, and braces are obtained with respect to FEMA and Iranian code number 360 [21]. Table 5 presents examples of criteria for braces with a circular hollow section. Component actions are classified in two categories: Deformation-controlled (DC) and Force-Controlled (FC). Some of the action types are shown in Table 6.

**Table 5. Deformation criteria for braces with a circular hollow section**

| Component/action   | Acceptance criteria                 |               |               |
|--|-------------------------------------|---------------|---------------|
|  | Plastic deformation (primary)       |               |               |
| Braces in compression                                    | IO                                  | LS            | CP            |
| $\frac{kl}{r} \geq 4.2\sqrt{E/F_{ye}}$                   | $0.25\Delta_c$                      | $5.0\Delta_c$ | $7.0\Delta_c$ |
| $\frac{kl}{r} \leq 2.1\sqrt{E/F_{ye}}$                   | $0.25\Delta_c$                      | $4.0\Delta_c$ | $6.0\Delta_c$ |
| $2.1\sqrt{E/F_{ye}} < \frac{kl}{r} < 4.2\sqrt{E/F_{ye}}$ | Linear interpolation shall be used. |               |               |
| Braces in tension  | $0.25\Delta_T$                      | $7.0\Delta_T$ | $9.0\Delta_T$ |

$\Delta_c$  is the axial deformation at expected buckling load

$\Delta_T$  is the axial deformation at expected tensile yielding load

**Table 6. Type of action for some elements**

| Action                            | Force-control    | Deformation-control |
|-----------------------------------|------------------|---------------------|
| Braces in tension and compression |                  | √                   |
| Columns compression               | √                |                     |
| Columns flexure                   | $p < 0.5 p_{cr}$ | √                   |
|                                   | $p > 0.5 p_{cr}$ | √                   |

In the process of calculating the modeling parameters of elements, most of beams and all of columns have been forced controlled (FC). For beams, due to d/t ratio, the modeling parameters and numerical acceptances are obtained. For FC

elements, for flexural component, the plastic moment capacity of the element is calculated ( $M_{CE} = zF_{ye}$ ) and assigned to the considered elements. Table 7 provides examples of criteria for beams with a circular hollow section.

**Table 7. Deformation criteria for beams with a circular hollow section**

| Component/action   | Acceptance criteria<br>Plastic deformation |               |               |
|--|--|---------------|---------------|
|  | IO   | LS            | CP            |
| Beams in flexure   |  |               |               |
| $\frac{d}{t} \leq 0.65 \sqrt{\frac{E}{F_{ye}}}$                                  | $1.0\theta_y$                              | $6.0\theta_y$ | $8.0\theta_y$ |
| $1.12 \sqrt{\frac{E}{F_{ye}}} \leq \frac{d}{t} \leq 1.4 \sqrt{\frac{E}{F_{ye}}}$ | $0.25\theta_y$                             | $2.0\theta_y$ | $3.0\theta_y$ |
| $0.65 \sqrt{\frac{E}{F_{ye}}} < \frac{d}{t} < 1.12 \sqrt{\frac{E}{F_{ye}}}$      | Linear interpolation shall be used.        |               |               |
| $\frac{d}{t} > 1.4 \sqrt{\frac{E}{F_{ye}}}$                                      | Force-control                              |               |               |

For columns, the modeling parameters are pertinent to both axial forces and flexures. The classification of the parameters is as same as beams with considering of the axial forces effects. Although all of columns had  $P/P_{cr} < 0.5$ , the d/D ratio of sections were bigger than the restraints for being DC elements ( $d/t > 1.4 \sqrt{E/F_{ye}}$ ). So, all of columns are FC and don't have any criteria like DC elements and are brittle. For finding parameters and criteria from the tables, calculating some parameters is essential.

For beams:

$$\theta_y = \frac{zF_{ye}l_b}{6EI_b} \quad (2)$$

$$M_{CE} = zF_{ye} \quad (3)$$

Where z is plastic section modulus; E is the modulus of elasticity;  $l_b$  and  $I_b$  are length and moment of inertia of beam;  $F_{yeb}$  is expected yield strength of material which is calculated by multiplying 1.1 by  $F_y$  (the yield strength of the material);  $\theta_y$  is the yield rotation; and  $M_{CE}$  is expected flexural strength. For columns:

$$\theta_y = \frac{zF_{ye}l_c}{6EI_c} \left[ 1 - \frac{P}{P_{ye}} \right] \quad (4)$$

$$M_{CE} = 1.18zF_{ye} \left[ 1 - \frac{P}{P_{ye}} \right] \leq zF_{ye} \quad (5)$$

Where  $l_c$  and  $I_c$  are length and moment of inertia of column; P is axial force in the member at the target displacement;  $P_{ye}$  is expected yield force of the member which is calculated by  $A_g F_{ye}$ .

$$P_{cr} = P_n = F_{cr} A_g \quad (6)$$

For calculating  $F_{cr}$ , due to the section type, the equations may be different. Since the columns have hollow circular sections, the limit state is flexural buckling [22].

$$\text{a) if } \frac{F_y}{F_e} \leq 2.25 \rightarrow F_{cr} = \left[ 0.658 \frac{F_{ye}}{F_e} \right] F_{ye} \quad (7)$$

$$\text{b) if } \frac{F_y}{F_e} > 2.25 \rightarrow F_{cr} = 0.877 F_e \quad (8)$$

Where  $A_g$  is gross cross-sectional area of member;  $F_e$  is elastic buckling stress ( $F_e = \pi^2 E / (kl_c/r)^2$ ); r is radius of gyration;  $F_{cr}$  is the critical stress; and  $P_n$  is the nominal compressive strength.

For braces, calculation of compression is as same as columns'. Equations for calculating the tension is presented below.

$$T_{CE} = F_{ye} A \quad (9)$$

$$\Delta_T = \frac{T_{CE}}{EA/l} \quad (10)$$

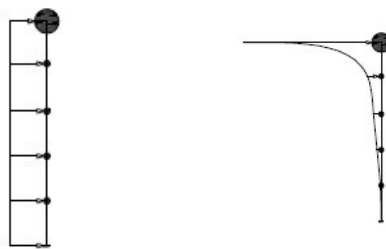
Where  $T_{CE}$  is expected axial strength in tension.

### 3- 1- Nonlinear pushover analysis

Non-linear pushover analysis is widely used for the assessment and rehabilitation of structures. It can be used to estimate the structural response under seismic loading. The target displacement of the structure is calculated for the deck level. The target displacement represents the maximum

displacement likely to be experienced by the structure during the design earthquake. The stresses and deformations of each element are evaluated at this displacement level.

Modal and constant pattern distribution of load shown in Figure 5 is applied for the pushover analysis. For considering the pushover analysis, gravitational loads are distributed first, then the modal or constant pattern distribution of load is applied where, in modal pattern, the first mode is in x-direction and the second one is in Y-direction. Moreover, according to FEMA 356, this load distribution is permitted only when more than 75% of the total mass participates in fundamental mode in the direction under consideration. Figure 6 shows the pushover curve of the structure in two directions. It represents that under modal pushover which is a more real loading pattern than constant one, the structure has lower capacity. The main damages will occur after about 0.5 m displacement.



a) Constant loading pattern      b) Modal loading pattern

Figure 5. Loading patterns

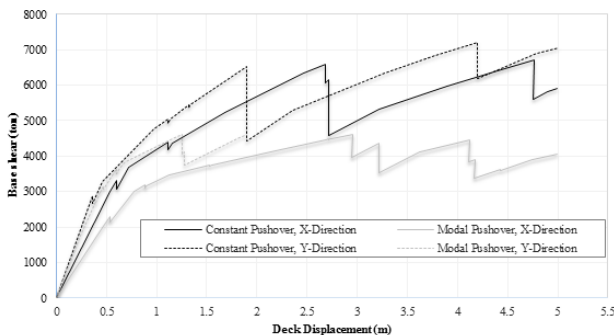


Figure 6. Pushover curve of SPD12

All of the elements are in operational (O) level representing the acceptable performance criteria in offshore platforms in the IO level, according to the API.

FEMA-356 and ATC-40 utilize the Coefficient Method and the Capacity-Spectrum Method respectively. In both methods, the response of an equivalent linear single-degree-of-freedom (SDOF) is estimated. These methods improved in the FEMA-440 document [23].

In the Coefficient Method, the maximum inelastic displacement (Target Displacement) is calculated from multiplying the linear elastic response by coefficients  $C_0$  through  $C_3$ . This method is depicted in Figure 7.  $T_1$ ,  $T_e$ ,  $k_p$ , and  $k_e$  are the elastic fundamental period, the effective fundamental period, the elastic lateral stiffness and the

effective lateral stiffness of the structure, respectively.

In the Capacity-Spectrum Method, the pushover plot which is the base shear versus roof displacement curve (capacity) and seismic ground motion (demand) are plotted in Acceleration-Displacement Response Spectrum (ADRS) format. The performance point (maximum in-elastic displacement) is the intersection point of demand and capacity. Figure 8 demonstrates this procedure.  $S_a$  and  $S_d$  are spectral acceleration and spectral displacement respectively.

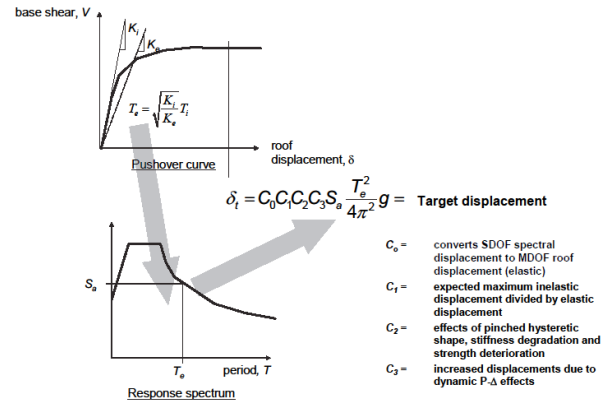


Figure 7. Coefficient method [23]

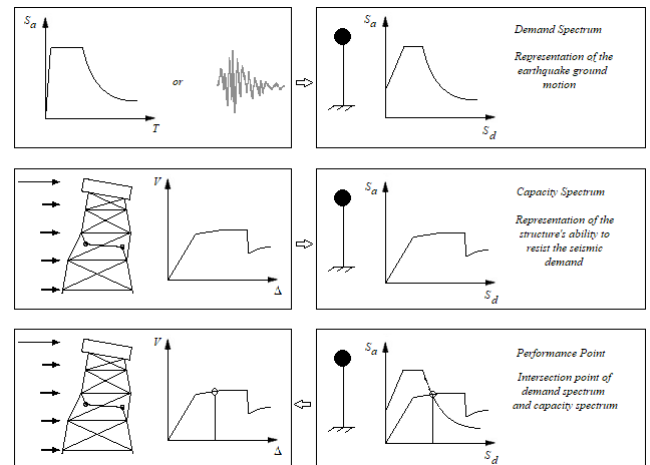
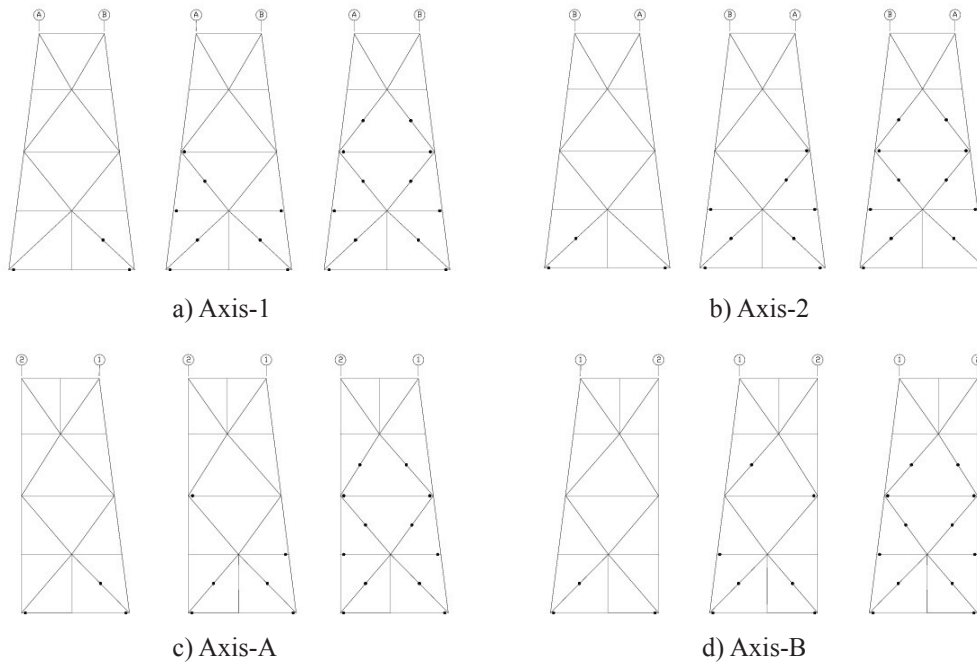


Figure 8. Capacity-spectrum method [7]

Due to the calculation with respect to ASCE 41, target displacement of the structure is about 30 cm in Y-direction and 40 cm in X-direction. As the results show, the structure passes the performance criteria in target displacement.

### 3- 2- Structure damage considering the seismic components

The damage distribution of all 4 frames are shown in Figures 9 and 10. In Figure 9, constant pattern pushover is considered. It is observed that the damage in jacket-type offshore SPD12 is distributed from the lowest part of the structure and damage is transmitting to the top levels of the structure in sequence by collapsing some elements of the lower part of that. Since most of the beams are FC, the results are shown that the main parts of the structure damaged are braces. Thus, the structural behavior of jacket-type platform is similar to a steel braced frame.



**Figure 9. Damage distribution of each frame under constant pattern pushover**

In contrast with constant pushover pattern, modal pushover pattern makes different damage distribution which is more reliable. So, results of this loading pattern can show better distribution. Figure 10 presents damage distribution in each frame of the structure. It is observed that damage is derived from the braces of the third floor and spread to 2<sup>nd</sup> and 4<sup>th</sup> floor. Due to modal loading pattern, lateral force is increasing

from bottom to top, therefore, the structure is under a bigger force on the top. This damage distribution is occurred since the shear force which is shown in Figure 11 is approximately equal for all stories, and due to the story stiffness which is stiffer in lower parts of the structure, shear force first causes damage in lower-stiffness story which is story three for SPD12.

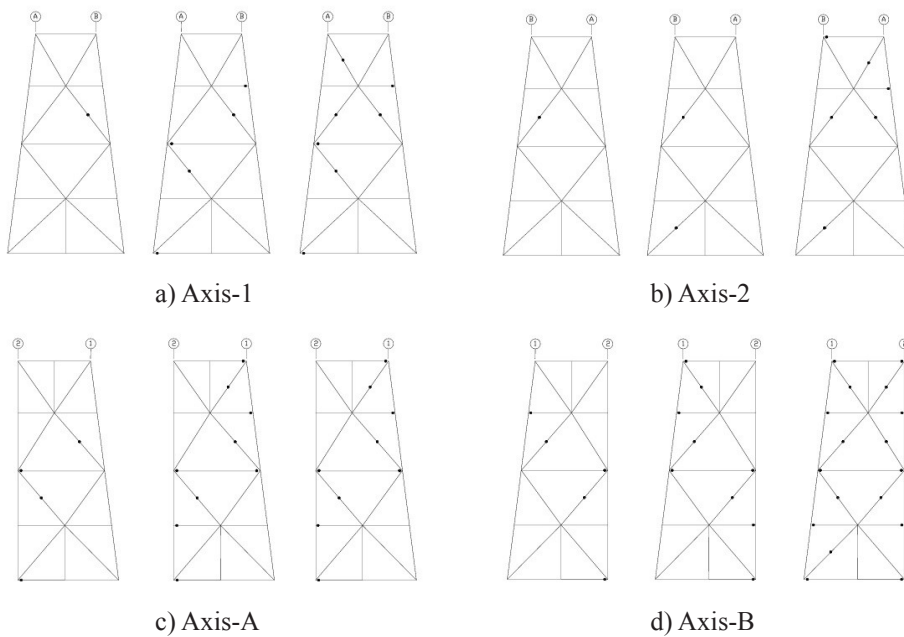


**Figure 10. Damage distribution of each frame under modal pattern pushover**



Figure 11. Comparison of shear force in each story due to loading pattern

#### 4- Conclusions

This study proposed a method to detect damage spread of a kind of offshore jacket-type platforms. A seismic assessment of the platform was considered to obtain distribution of plastic hinges due to pushover analysis. As an example, an existing 4-legged jacket-type platform SPD12 was assessed with FEMA-356. This research is shown that:

- In jacket-type platform which has  $\wedge$  and  $\vee$  braces, damages are distributed from the lower-stiffness part of the structure like every structure. In constant pushover loading pattern, damage is being distributed from the lower story where shear force is very great, and in modal pushover loading pattern, damage is being spread from the 3<sup>rd</sup> floor where the ratio of shear force to stiffness is much greater.
- Damage spread of the structure shows that the structural behavior of a jacket-type platform is very similar to a steel braced frame since main damages are propagated from braces. Therefore, the structure will have the same function as a steel braced frame.
- Knowing spread of damages will help to reinforce some parts of the structure where will be damaged first and enhance the capacity of the structure, or make the design more cost-effective with respect to optimization of the structure due to the damage distribution.

#### Declaration of interest

The authors report no conflicts of interest. The authors alone are responsible for the content and writing of this article.

#### References

- [1] S. Malekpour, P. Seyyedi, F. Dashti, J.F. Asghari, Seismic performance evaluation of steel moment-resisting frames using Iranian, European and Japanese seismic codes, *Procedia Engineering*, 14 (2011) 3331-3337.
- [2] P. Sultana, M.A. Youssef, Prediction of local seismic damage in steel moment resisting frames, *Journal of Constructional Steel Research*, 122 (2016) 122-137.
- [3] D.P. McCrum, A. Staino, Seismic damage detection for a steel braced frame structure, *Proceedings of the Institution of Civil Engineers-Structures and Buildings*, 168(9) (2015) 636-648.
- [4] S. Gholizadeh, H. Poorhoseini, Performance-Based Optimum Seismic Design of Steel Dual Braced Frames by Bat Algorithm, in: *Metaheuristics and Optimization in Civil Engineering*, Springer, 2016, pp. 95-114.
- [5] W. Krieger, H. Banon, J. Lloyd, R. De, K. Digre, D. Nair, J. Irick, S. Guynes, Process for assessment of existing platforms to determine their fitness for purpose, in: *Offshore Technology Conference*, Offshore Technology Conference, 1994.
- [6] A. Golafshani, M. Tabeshpour, Y. Komachi, Assessment and retrofit of existing jacket platform using friction damper devices, in: *8th International Conference of Ocean Industries*. Bushehr University, Bushehr, Iran (in Persian), 2006.
- [7] A.A. Golafshani, M.R. Tabeshpour, Y. Komachi, FEMA approaches in seismic assessment of jacket platforms (case study: Resselat jacket of Persian gulf), *Journal of Constructional Steel Research*, 65(10-11) (2009) 1979-1986.
- [8] J.-T. Kim, N. Stubbs, Damage detection in offshore jacket structures from limited modal information, *International Journal of Offshore and Polar Engineering*, 5(01) (1995).
- [9] H. Yang, H. Li, S.-L. Hu, Damage localization for offshore structures by modal strain energy decomposition method, in: *American Control Conference*, 2004. *Proceedings of the 2004, IEEE*, 2004, pp. 4207-4212.
- [10] X. Shi, T. Matsui, H.J. Li, C. Gong, A damage detection algorithm based on partial measurement for offshore jacket platforms, in: *The Seventeenth International Offshore and Polar Engineering Conference*, International Society of Offshore and Polar Engineers, 2007.
- [11] A.A. Elshafey, M.R. Haddara, H. Marzouk, Damage detection in offshore structures using neural networks, *Marine Structures*, 23(1) (2010) 131-145.
- [12] B. Asgarian, M. Amiri, A. Ghafooripour, Damage detection in jacket type offshore platforms using modal strain energy, *Structural Engineering and Mechanics*, 33(3) (2009) 325-337.
- [13] B. Asgarian, V. Aghaeidoost, H.R. Shokrgozar, Damage detection of jacket type offshore platforms using rate of signal energy using wavelet packet transform, *Marine Structures*, 45 (2016) 1-21.
- [14] Structural report of wellhead platform SPD12, SP12-24-D-23-5-001/D3, South Pars Gas Field Development Phase 12, 2010.
- [15] CSI, Sap2000: V11. 0 Integrated Software for Structural Analysis and Design, (2004).
- [16] API, Recommended practice for planning, designing, and constructing fixed offshore platforms, in, *American Petroleum Institute*, 1989.
- [17] M.A. Lotfollahi-Yaghin, H. Ahmadi, H. Tafakhor, Seismic responses of an offshore jacket-type platform incorporated with tuned liquid dampers, *Advances in Structural Engineering*, 19(2) (2016) 227-238.
- [18] Y. Toyama, Drift-wood collision load on bow structure of high-speed vessels, *Marine Structures*, 22(1) (2009) 24-41.

- [19] FEMA, Commentary for the seismic rehabilitation of buildings, in: FEMA-356, Federal Emergency Management Agency, Washington, DC, 2000.
- [20] C.D. Comartin, R.W. Niewiarowski, C. Rojahn, Seismic evaluation and retrofit of concrete buildings, Seismic Safety Commission, State of California, 1996.
- [21] S. 360, Iranian code of instructions on seismic reconstruction of existing buildings, in, Building and Housing Research Center, Tehran, Iran, 2012.
- [22] AISC, AISC 360–16.(2016), in: Specification for structural steel buildings.
- [23] FEMA, 440, Improvement of nonlinear static seismic analysis procedures, in: FEMA-440, Redwood City, 2005.

Please cite this article using:

M. Aghajani Delavar, K. Bargi, Prediction of Local Seismic Damage in Jacket-type Offshore Platforms, *AUT J. Civil Eng.*, 2(2) (2018) 241-250.

DOI: 10.22060/ajce.2018.14738.5495



